Makino, K., Morimoto, M., Nishi, M., Sakamoto, S., Tamura, A., Inooka, H., & Akasaka, K. (1987) *Proc. Natl. Acad. Sci. U.S.A. 84*, 7841–7845.
Martin, B. L., Wu, D., Tabatabi, L., & Graves, D. J. (1990) *Arch. Biochem. Biophys. 276*, 94–101.
McFadden, P. N., & Clarke, S. (1986) *J. Biol. Chem. 261*, 11503–11511.
McFadden, P. N., & Clarke, S. (1987) *Proc. Natl. Acad. Sci. U.S.A. 84*, 2595–2599.
Momand, J., & Clarke, S. (1987) *Biochemistry 26*, 7798–7805.
Murray, E. D., Jr., & Clarke, S. (1984) *J. Biol. Chem. 259*, 10722–10732.
Oka, Y., & Orth, D. N. (1983) *J. Clin. Invest. 72*, 249–259.
O'Keefe, J. H., Fifis, T., Bender, V. J., & Moss, B. A. (1984) *J. Chromatogr. 25*, 45–59.
Ota, I., & Clarke, S. (1989a) *Biochemistry 28*, 4020–4027.
Ota, I., & Clarke, S. (1989b) *J. Biol. Chem. 264*, 54–60.
Ota, I., Ding, L., & Clarke, S. (1987) *J. Biol. Chem. 262*, 8522–8531.
Petrides, P. E., Böhlen, P., & Shively, J. E. (1984) *Biochem. Biophys. Res. Commun. 125*, 218–228.
Savage, C. R., Jr., Inagami, T., & Cohen, S. (1972) *J. Biol. Chem. 247*, 7612–7621.
Savage, C. R., Jr., Hash, J. H., & Cohen, S. (1973) *J. Biol. Chem. 248*, 7669–7672.
Schultz, J. (1967) *Methods Enzymol. 11*, 255–263.
Simpson, R. J., Smith, J. A., Moritz, R. L., O'Hare, M. J., Rudland, P. S., Morrison, J. R., Lloyd, C. L., Grego, B., Burgess, A. W., & Nice, E. C. (1985) *Eur. J. Biochem. 153*, 629–637.
Smith, J., Cook, E., Fotheringham, I., Pheby, S., Derbyshire, R., Eaton, M. A. W., Doel, M., Lilly, D. M., Pardon, J. F., Patel, T., Lewis, M., & Bell, L. D. (1982) *Nucleic Acids Res. 10*, 4467–4482.
Smith, J. A., Ham, J., Winslow, D. P., O'Hare, M. J., & Rudland, P. S. (1984) *J. Chromatogr. 305*, 295–308.
Stephenson, R. C., & Clarke, S. (1989) *J. Biol. Chem. 264*, 6164–6170.
Travis, J., Owen, M., George, P., Carrel, R., Rosenberg, S., Hallewell, R. A., & Barr, P. J. (1985) *J. Biol. Chem. 260*, 4384–4389.

Folding of a Predominantly β-Structure Protein: Rat Intestinal Fatty Acid Binding Protein†

Ira J. Ropson,‡ Jeffrey I. Gordon,‡,§ and Carl Frieden*,‡
Department of Biochemistry and Molecular Biophysics and Department of Medicine, Washington University Medical School, St. Louis, Missouri 63110
Received June 20, 1990

ABSTRACT: The equilibrium and kinetic properties of the unfolding–refolding transitions of *Escherichia coli* derived rat intestinal fatty acid binding protein have been examined using several different denaturants. This protein, which contains 2 tryptophans but no prolines or cysteines, has a predominantly β-structure: its 10 antiparallel β-strands are organized into 2 orthogonal sheets surrounding a large solvent-filled internal cavity. For urea and guanidine hydrochloride, the completely reversible transition was monitored by circular dichroism, absorbance, and fluorescence spectroscopy. Each of these data sets was best fit by a simple, two-state model involving only native and unfolded forms. However, linear extrapolation to determine the free energy of folding in the absence of denaturant resulted in different values for the free energy of folding depending upon which denaturant was used. When fluorescence was used to monitor the transition, the extrapolated free energy estimates for the two denaturants were markedly different: 10.03 ± 0.24 kcal mol^{-1} for urea versus 5.22 ± 0.33 kcal mol^{-1} for guanidine hydrochloride. The midpoints of these transitions were 5.51 and 1.36 M, respectively. The transition caused by either denaturant as monitored by circular dichroism and absorbance spectroscopy was virtually coincident with that monitored by fluorescence, further supporting the assignment of a two-state model for the equilibrium results. The addition of a 2-fold molar excess of ligand (oleate) increased the extrapolated estimates approximately 2.5 kcal mol^{-1} for both denaturants. Stop-flow kinetic studies of the guanidine hydrochloride induced transitions showed that the unfolding and folding processes are rapid (complete in less than a minute under the slowest conditions) and complex, indicating the presence of intermediates on both pathways. The unfolding process was biphasic: the two phases accounted for the entire amplitude of the transition, suggesting that some type of sequential unfolding of the protein occurs. Two phases were also observed for the folding reaction, but at least one additional phase must occur in the dead time of the instrument (<10 ms) to account for the expected amplitude change. The changes in the amplitudes of the folding phases suggest the existence of multiple pathways for the folding of rat intestinal fatty acid binding protein and that the proportion of protein molecules following any particular pathway is dependent on the final denaturant concentration.

One of the fundamental questions of biochemistry is how the primary sequence of a protein encodes the information leading to the formation of an organized structure capable of function. Although considerable progress has been made, particularly for a few carefully studied proteins, the general rules of protein folding have not been determined. This is particularly true for proteins that consist primarily of β-sheet structure, since so few have been examined. This paper begins

† Supported by NIH Grants DK13332 to C.F. and DK30292 to J.I.G.
* Author to whom correspondence should be addressed.
‡ Department of Biochemistry and Molecular Biophysics.
§ Department of Medicine.

0006-2960/90/0429-9591$02.50/0

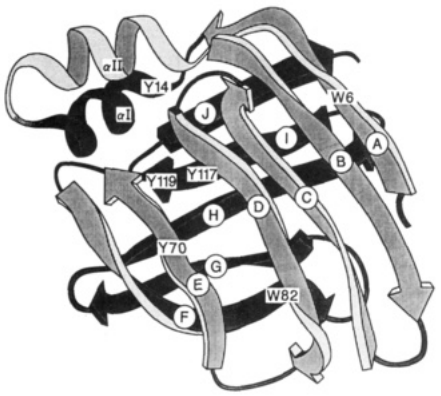

FIGURE 1: Ribbon drawing showing the backbone tracing and the location of the two tryptophans and four tyrosines of IFABP.

to address the folding of an all-β-type protein that has several inherent advantages as a model system, rat intestinal fatty acid binding protein (IFABP).[1]

Escherichia coli derived IFABP is a monomeric protein of 131 amino acids (15 107 daltons).[2] There are no cysteines or prolines, thereby avoiding two of the major problems that complicate the analysis of protein folding, namely, irreversible intra- and intermolecular cross-linking by the formation of incorrect disulfide bonds (Baldwin, 1989) and the slow cis–trans isomerization of proline (Brandts et al., 1975). The locations of the four tyrosines and two tryptophans of IFABP, providing potential optical probes for different regions of the protein, are shown in Figure 1.

This cytoplasmic protein is thought to participate in the uptake of long-chain fatty acids into intestinal absorptive cells (enterocytes) and/or the delivery of fatty acids to sites of metabolic processing [reviewed in Sweetser et al. (1987)]. It is a member of a family of small homologous cytoplasmic hydrophobic ligand binding proteins. Other family members include heart and liver fatty acid binding proteins (Heuckeroth et al., 1987; Gordon et al., 1983), cellular retinol binding proteins I and II (Sundelin et al., 1985a; Li et al., 1986), cellular retinoic acid binding protein (Sundelin et al., 1985b), adipocyte and Schwann cell specific proteins aP2 and P2 (Bernlohr et al., 1984; Hunt et al., 1985; Ishaque et al., 1987), mammary gland protein (Böhmer et al., 1987), and porcine ileal protein (Walz et al., 1988).

Rat IFABP cDNA has been placed into several prokaryotic expression vectors (Lowe et al., 1987; Sacchettini et al., 1990). After induction, this mammalian protein represents as much as 15% of the total soluble protein in *E. coli* (Sacchettini et al., 1990). X-ray crystallographic studies have defined the tertiary structures of *E. coli* derived rat IFABP without ligand to 1.96-Å resolution (Sacchettini et al., 1989a) and to 2.0-Å resolution with bound palmitate (Sacchettini et al., 1989b). The noncovalent binding of its single ligand molecule has very little effect on the tertiary structure (Sacchettini et al., 1989b). The protein consists of 2 nearly orthogonal β-sheets formed by 10 antiparallel β-strands (βA–βJ, Figure 1). Two short helices (αI and αII, Figure 1) are interposed between βA and βB. The enclosed cavity of this structure serves as the binding site for ligand. The structure resembles a clam shell and has been called a "β-clam" (Sacchettini et al., 1988). The conformation of the other member of this family whose structure has been solved, bovine P2 protein, is very similar (Jones et al., 1988). This β-clam conformation also resembles that of several extracellular hydrophobic ligand binding proteins that bind their ligands within an eight-stranded β-barrel: e.g., serum retinol binding protein (Newcomer et al., 1984), bilin binding protein/insecticyanin (Huber et al., 1987), and β-lactoglobulin (Monaco et al., 1987).

In this paper, we report the equilibrium properties of the GdnHCl- and urea-induced reversible unfolding transition in IFABP, along with some information for the unfolding transition using dimethylurea, KSCN, and GdnSCN as denaturants. Further, we show the kinetic properties of the GdnHCl-induced unfolding and refolding transitions. From these data, we speculate on possible folding mechanisms.

Materials and Methods

Protein Source and Purification. The purification of IFABP produced in *E. coli* by using an expression vector containing the leftward promoter from phage λ has been described elsewhere (Lowe et al., 1987; Sacchettini et al., 1987). More recently, a second expression system (Olins & Rangwala, 1990) has been used to increase the levels of expression still further (Sacchettini et al., 1990). The isolation procedures were identical for both expression systems and yielded preparations of protein that exhibited no differences for any physical parameters or in their folding behavior.

Purified IFABP was delipidated by using a previously described protocol (Lowe et al., 1987; Sacchettini et al., 1989a, 1990). Protein purity was demonstrated by the observation of a single band on $NaDodSO_4$, native and isoelectric focusing polyacrylamide gels. IFABP concentration was typically measured by the absorbance at 280 nm, using an extinction coefficient of 1.18 mg^{-1} cm^{-1}. Alternatively, when GdnHCl was present in denaturing concentrations, protein concentration was calculated on the basis of the content of tyrosine, tryptophan, and phenylalanine residues, as described by Johnson (1988). Good agreement was found for both methods with that calculated from amino acid analysis.

Spectroscopic Methods. Equilibrium unfolding as a function of denaturant concentration was monitored by three spectroscopic techniques: (1) UV difference spectroscopy, where changes at 287 and 292 nm were measured with a Cary 118 spectrophotometer or over the wavelength range from 250 to 300 nm with a Hewlett Packard 8151A diode array spectrophotometer; (2) circular dichroism (CD) by following the loss of secondary structure in the 225–212-nm range using either a 1-mm or a 0.1-mm cell in a Jasco J-600 spectropolarimeter interfaced with an IBM PS2 Model 50 computer; or (3) fluorescence spectroscopy with excitation at 290 nm (5-nm band-pass) and monitoring the emission at 330 nm (40-nm band-pass, wavelength of greatest change) and 338 nm (40-nm band-pass, peak emission wavelength of the native protein) on a SPEX Fluorolog fluorometer. All samples were equilibrated at the appropriate denaturant concentration at 20 °C before measurements were made. The change in each optical parameter was examined at several different protein concentrations. The ranges examined were 20–50 μM for absorbance changes, 6–35 μM for CD changes, and 1–7 μM for fluorescence changes.

Kinetics of folding were followed by UV difference spectroscopy and fluorescence using an Applied Photophysics stop-flow spectrophotometer (Model SFMV12) interfaced with

[1] Abbreviations: IFABP, rat intestinal fatty acid binding protein; GdnHCl, guanidine hydrochloride; $NaDodSO_4$, sodium dodecyl sulfate; CD, circular dichroism; KSCN, potassium thiocyanate; GdnSCN, guanidine thiocyanate; ΔG_{H_2O}, free energy of unfolding in the absence of denaturant.

[2] The primary translation product of IFABP mRNA contains 132 residues. The initiator Met of IFABP is efficiently removed in *E. coli*, leaving Ala^2 as the NH_2-terminal amino acid (Lowe et al., 1987). IFABP isolated from rat intestine has a blocked NH_2 terminus: it is not known if the blocking group is attached to the Met^1 or the Ala^2 residue.

an Archimedes 420 (Acorn) computer. UV difference measurements were made at 292, 290, and 287 nm (2-mm slits) with a 1-cm light path at 20 °C. Fluorescence measurements were made by exciting at 290 nm (2-mm slits) using a 0.2-cm path length and monitoring the emission intensity above 305 nm at 90° with a WG305 Schott glass filter (Oriel) at 20 °C. A wide range of final denaturant concentrations was achieved thorugh the use of several different size drive syringes to obtain different mixing ratios. Although the measured dead time of the Applied Photophysics instrument is less than 2 ms for solutions of similar composition (Paul et al., 1980; Tonomura et al., 1978), the large differences in refractive index and density between solutions containing or lacking denaturant caused an artifact for the first 10–50 ms of all runs, depending on the mixing ratio. The duration of the artifact was measured by mixing solutions with the same concentration of denaturant but lacking protein. Very large mixing ratios resulted in longer dead times. Data collected in the time range of the artifact were discarded from the analysis.

Kinetic measurements of refolding were also monitored by CD at 216 nm in a Jasco J-600 spectrophotometer using the Jasco SFC-5 stop-flow apparatus. Due to the severe limitations of the apparatus, only 1:1 ratio mixing could be performed: a lens system was required to focus light through the cell (details available on request), and a mixing artifact was observed for the first 100 ms of each transient. When a 1-cm path-length observation cell was used, a minimum of 24 transient accumulations had to be collected to obtain usable data.

Computer Fitting of Equilibrium and Kinetic Data. Nonlinear least-squares fits to the equilibrium data were obtained by using the Statistical Analysis Systems program NLIN (Sas Institute Inc., Cary, NC) and the following equation adapted from Santoro and Bolen (1988):

$$X_{[D]} = \{(X_N + m_N[D]) + (X_U + m_U[D]) \exp[-(\Delta G_{H_2O}/RT + m_G[D]/RT)]\}/\{1 + \exp[-(\Delta G_{H_2O}/RT + m_G[D]/RT)]\}$$

where $X_{[D]}$ is the value of the spectroscopic property at some denaturant concentration, X_N and X_U are the values for the spectroscopic property linearly extrapolated to [D] = 0 for the native and unfolded forms of the protein, respectively, m_N and m_U are the slopes for the dependence of the spectroscopic properties X_N and X_U on denaturant concentration, respectively, ΔG_{H_2O} is the apparent free energy difference between the folded and unfolded forms of the protein linearly extrapolated to [D] = 0, m_G is the slope describing the dependence of ΔG_{H_2O} on [D], assuming a linear relationship between the log of the equilibrium constant and denaturant concentration, R is the gas constant, and T is the temperature. The midpoint of the transition was determined by dividing ΔG_{H_2O} by $-m_G$. Goodness of fit to the various models was assessed by the criteria of Mannervik (1982) and Motulsky and Ransas (1989). If the standard error of a parameter exceeded the value of that parameter determined by fitting, the parameter was eliminated from the above equation, and the fit was repeated. This process of elimination was continued until all remaining terms were significant. No fits to any data set were significantly improved by the addition of terms representing the presence of any stable intermediates.

In order to easily compare the effects of different denaturants on fluorescence, the data for each denaturant were scaled from 0 to 1 by using the equation:

$$F_{rel} = (F - F_{min})/(F_{max} - F_{min})$$

where F_{rel} is the relative fluorescence, F is the observed fluorescence, and F_{max} and F_{min} are the maximum and minimum observed fluorescence for that data set, respectively.

The program supplied by Applied Photophysics was used to determine the nonlinear least-squares fits of the kinetic data to the equation:

$$A(t) = \sum^{i} A_i \exp(-k_i t) + A_\infty$$

where $A(t)$ is the amplitude of the change at time t, A_∞ is the amplitude at infinite time, A_i is the amplitude at zero time of phase i, and k_i is the rate of phase i. Goodness of fit to the various models was assessed by the criteria of Mannervik (1983) and Motulsky and Ransas (1989), as described above. Additional phases were added to the equation until no significant improvement in the residual sum of squares was observed. Some of these data sets were fit to the same equation by nonlinear least-squares regression with the NLIN program described above. No significant differences were found for the parameters determined by the different fitting algorithms. The values for A_∞ at a particular protein concentration were used to construct an equilibrium transition profile so that the expected fluorescence change for any refolding or unfolding jump could be calculated.

Reagents. Urea, dimethylurea, and GdnHCl stock solutions used in refolding experiments were made as 8, 8, and 6 M stocks, respectively, prepared by dissolving ultrapure urea, GdnHCl (Schwarz/Mann), or reagent-grade dimethylurea (Sigma) in distilled, deionized water. Urea and dimethylurea solutions were deionized by adding 1 g of mixed-bed resin (Bio-Rad AG 501-X8) per 150 g of denaturant and stirring at room temperature for 1 h. KSCN and GdnSCN solutions were prepared as 8.5 and 4 M stocks, respectively, by dissolving the reagent-grade chemicals in distilled, deionized water. All stock solutions were filtered through a 0.4-μm Millipore filter and stored at −70 or −20 °C. Urea, dimethylurea, and GdnHCl concentrations were determined by refractive index measurements using an Abbe refractometer at 25 °C and equations relating refractive index to concentration (Pace, 1986; Santoro & Bolen, 1988). Oleic acid was from Nucheck. All other chemicals were reagent grade. The buffer used for all experiments contained 20 mM potassium phosphate and 0.1 mM EDTA, adjusted to pH 7.2 at 20 °C, and were filtered through a 0.4-μm filter immediately before use.

Results

Equilibrium Studies of Apo- and Holo-IFABP. The urea- and GdnHCl-induced unfolding transition of *E. coli* derived apo-IFABP (i.e., without bound fatty acid) were followed by difference UV, CD, and fluorescence spectroscopy at several different wavelengths. The transition curves obtained by these methods were coincident for each denaturant. The dimethylurea-, GdnSCN-, and KSCN-induced unfolding transitions were observed by fluorescence only.

The change in the extinction coefficient at 292 nm is shown in panel A of Figure 2 for the GdnHCl-induced transition. There is little if any effect of GdnHCl on the extinction coefficient in the pretransition zone, but there is a significant effect on the extinction coefficient of the denatured protein. Similarly, there is little effect of GdnHCl on the molar ellipticity at 216 nm of native IFABP, whereas a larger effect is found on the denatured protein at this wavelength (Figure 2B). Finally, the transition monitored by the fluorescence emission at 338 nm (excitation 290 nm) is shown in Figure 2C. There is little effect of denaturant on the fluorescence of either the native or the denatured states. The sigmoidal change in these optical parameters between 1 and 1.8 M

Table I: Parameters Characterizing the Fits of the Equilibrium Unfolding Transition of IFABP under Various Conditions

denaturant (probe)[a]	X_N[b]	m_N[b] (M^{-1})	X_U[b]	m_U[b] (M^{-1})	ΔG_{H_2O}[b] (kcal mol^{-1})	m_G[b] (kcal mol^{-1} M^{-1})	midpoint[b] (M)
			Apo-IFABP				
dimethylurea (F_{352})	0[c]	0.02 ± 0.01	0.88 ± 0.04	0.02 ± 0.01	9.71 ± 0.43	−1.81 ± 0.21	5.36
GdnHCl (ϵ_{292})	12.58 ± 0.05	0	8.74 ± 0.15	0.31 ± 0.05	5.55 ± 0.49	−4.24 ± 0.38	1.31
GdnHCl (θ_{216})	−11631 ± 56	0	−4093 ± 151	441 ± 49	5.84 ± 0.23	−4.47 ± 0.18	1.31
GdnHCl (F_{338})	0.95 ± 0.02	0.07 ± 0.04	0	0	5.22 ± 0.33	−3.82 ± 0.21	1.36
GdnHCl (F_{305}), stopflow	0.94 ± 0.03	0.05 ± 0.04	0	0.01 ± 0.002	5.71 ± 0.41	−4.32 ± 0.28	1.32
GdnSCN (F_{338})	0.99 ± 0.01	−0.32 ± 0.03	0.18 ± 0.06	−0.15 ± 0.05	10.21 ± 0.58	−13.98 ± 0.81	0.73
KSCN (F_{338})	1.00 ± 0.01	0	0.34 ± 0.03	−0.04 ± 0.01	4.69 ± 0.23	−1.39 ± 0.07	3.37
urea (ϵ_{292})	12.70 ± 0.10	0	8.33 ± 0.20	0	10.25 ± 0.51	−1.85 ± 0.22	5.55
urea (θ_{216})	−10971 ± 101	0	−3655 ± 245	319 ± 66	9.63 ± 0.81	−1.77 ± 0.33	5.43
urea (F_{338})	0.98 ± 0.01	0	0	0	10.03 ± 0.24	−1.82 ± 0.04	5.50
urea (F_{338})[d] + 1 M NaCl	1.00 ± 0.01	0	0	0	9.71 ± 0.54	−1.85 ± 0.10	5.25
			Holo-IFABP				
GdnHCl (F_{338})	0.99 ± 0.01	−0.02 ± 0.01	0	0	7.86 ± 0.28	−5.22 ± 0.18	1.51
urea (F_{338})	0.98 ± 0.01	0	0	0	12.55 ± 0.29	−2.17 ± 0.05	5.79

[a] All solutions contained 20 mM potassium phosphate and 0.1 mM EDTA adjusted to pH 7.2 at 20 °C. F_{338}, F_{352} and F_{305} represent the relative fluorescence intensity in arbitrary units at 338 nm, 352 nm, of or at wavelengths >305 nm, as described under Materials and Methods. ϵ_{292} represents the extinction coefficient at 292 nm and θ_{216} the mean residue ellipticity at 216 nm. [b] X_N and X_U are the values of the specified optical parameter for native and unfolded protein extrapolated to 0 M denaturant, respectively. m_N and m_U are slope terms describing the dependence of X_N and X_U on denaturant concentration. ΔG_{H_2O} is the apparent free energy difference between the folded and unfolded forms of IFABP extrapolated to 0 M denaturant. m_G is the slope describing the dependence of ΔG on denaturant concentration. The midpoint is the denaturant concentration at the midpoint of the transition. [c] The fitted value of this parameter under these conditions was not significantly different from 0. [d] This denaturant profile contained 1 M NaCl at all concentrations of urea.

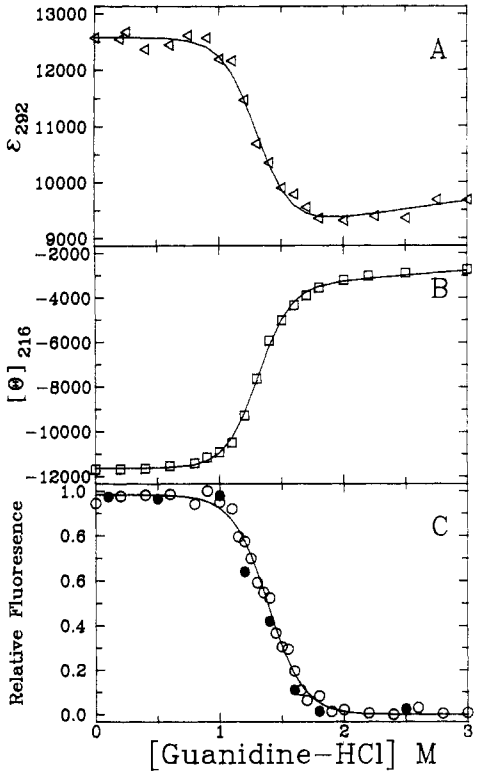

FIGURE 2: Equilibrium unfolding of apo-IFABP monitoring GdnHCl-induced unfolding by (A) the tryptophan absorbance at 292 nm (△), (B) the molar ellipticity at 216 nm (□), and (C) the tryptophan fluorescence at 338 nm, excited at 290 nm (○, ●). The solvent for all studies contained 20 mM potassium phosphate and 0.1 mM EDTA, adjusted to pH 7.2 at 20 °C. The apo-IFABP concentrations were 46, 6.6, and 3 μM for panels A, B, and C, respectively. The lines indicate the fits to a two-state model, as described under Materials and Methods. The reversibility of the transition was shown by incubating IFABP in 5 M GdnHCl overnight to ensure complete unfolding and then diluting the solution to the final GdnHCl concentrations shown in panel C (●).

GdnHCl can be attributed to the cooperative unfolding of the protein over this concentration range. The lines shown are the fits to a two-state model, assuming a linear dependence of the free energy of folding on the GdnHCl concentration.

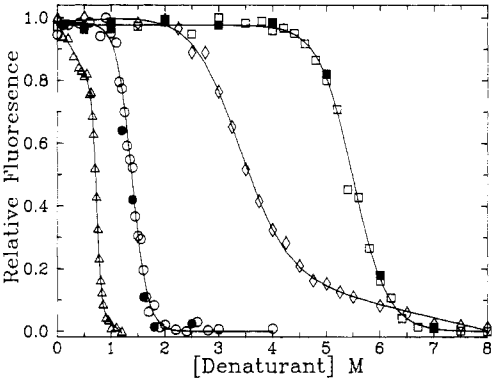

FIGURE 3: Equilibrium unfolding of apo-IFABP monitored by fluorescence for the GdnSCN- (△), GdnHCl- (○, ●), KSCN- (◇), and urea-induced (□, ■) unfolding transition. Open symbols represent the dilution of IFABP in buffer to the final concentration of denaturant shown. Closed symbols show the reversibility of the transition where IFABP was equilibrated in 5 M GdnHCl or 8 M urea overnight and diluted to the final concentrations of denaturant shown. All solutions contained 3.3 μM IFABP, 20 mM potassium phosphate, and 0.1 mM EDTA, adjusted to pH 7.2 at 20 °C. The lines indicate the fits to a two-state model, as described under Materials and Methods.

The free energy of unfolding in the absence of GdnHCl calculated by nonlinear regression was 5.55 ± 0.49 kcal mol^{-1} by difference UV, 5.84 ± 0.23 kcal mol^{-1} from changes in molar ellipticity, and 5.22 ± 0.33 kcal mol^{-1} by changes in fluorescence intensity at pH 7.2 and 20 °C. The values for the other fitting parameters are shown in Table I. Considering the intrinsic errors involved in these measurements and calculations, it is highly unlikely that there are any significant differences in the transition curves monitored by these methods. Observations of the transitions by these methods at other wavelengths and at several different protein concentrations gave virtually identical profiles. The transition caused by GdnHCl was completely reversible for all optical parameters (data shown only for the fluorescence transition, Figure 2C).

The unfolding transitions caused by urea, KSCN, GdnSCN, and GdnHCl as monitored by fluorescence are compared in Figure 3. In all cases, the transition was completely reversible, and IFABP was in an unfolded state by CD spectral criteria (loss of peak ellipticity at 216 nm) at posttransition concen-

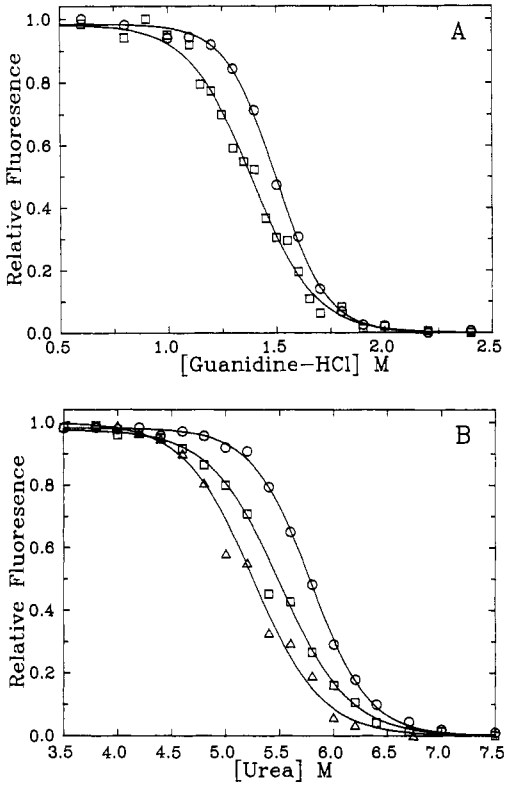

FIGURE 4: (A) Equilibrium unfolding of IFABP monitored by fluorescence for the GdnHCl-induced unfolding transition in the absence (□) or presence (○) of a 2-fold molar excess of oleate. (B) Equilibrium unfolding of IFABP monitored by fluorescence for the urea-induced unfolding transition without additions (□), with a 2-fold molar excess of oleate (○), or in the presence of 1 M NaCl (△). Other conditions are identical with those described in Figure 3. The lines indicate the fits to a two-state model, as described under Materials and Methods.

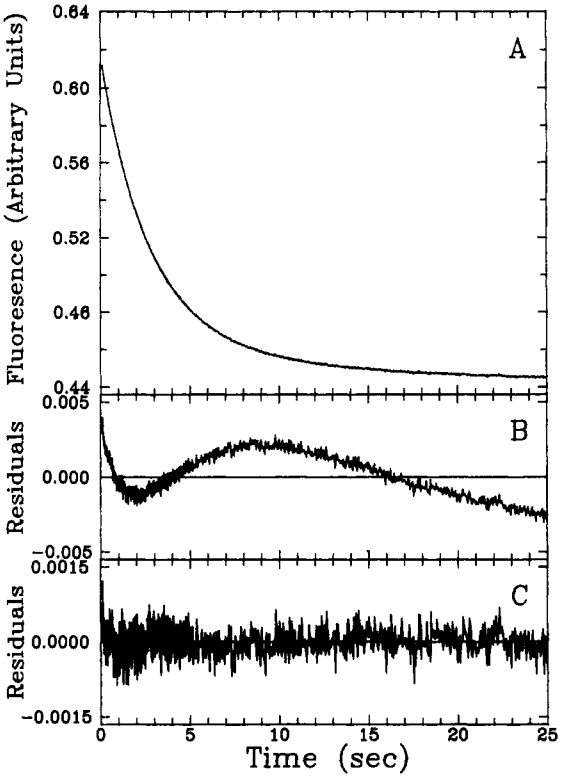

FIGURE 5: (A) Plot of the change in fluorescence intensity vs time for an unfolding jump from 0 to 2 M GdnHCl measured by stopped-flow. The tryptophans were excited at 290 nm using a 2 mm light path, and the emitted light was monitored at wavelengths above 305 nm. Two different volume drive syringes were used. The protein syringe (0.5-mL volume) contained 120 μM apo-IFABP, 20 mM potassium phosphate, and 0.1 mM EDTA, pH 7.2, while the other syringe (2.5-mL volume) contained 2.4 M GdnHCl, 20 mM potassium phosphates, and 0.1 mM EDTA at pH 7.2. This mixing ratio resulted in a final concentration of 20 μM apo-IFABP and 2 M GdnHCl. The first 50 ms was discarded from the analysis. (B) and (C) are plots of the residuals of the fits to one and two exponentials, respectively.

trations of denaturant. These denaturants have remarkably varied effects on the fluorescence of both native and unfolded apo-IFABP, as shown by the slopes in the pre- and posttransition regions (m_U and m_N, Table I). Significant differences were found for the free energy of unfolding for the different denaturants (see Table I). Possible reasons for these unusually large differences for ΔG_{H_2O} among the different denaturants are discussed later.

One possible explanation for the differences in free energy of unfolding between the ionic (GdnHCl, KSCN) and the nonionic denaturants (urea, dimethylurea) is the high ionic strength of the solutions containing ionic denaturants. In order to determine if high ionic strength was responsible for a portion of these differences, 1 M NaCl was added to the buffer for a urea unfolding transition. However, the effects of this concentration of NaCl were slight and do not account for the observed differences in free energy of unfolding among the denaturants (Figure 4B, Table I).

The effects of ligand on the unfolding transition are shown in Figure 4. The presence of a 2-fold molar excess of ligand (oleate) led to an increase in ΔG_{H_2O} of about 2.5 kcal mol^{-1} when either GdnHCl (ΔG_{H_2O} = 7.86 kcal mol^{-1}) or urea (ΔG_{H_2O} = 12.55 kcal mol^{-1}) was used as the denaturant. The presence or absence of ligand did not effect the 5 kcal mol^{-1} difference between these two denaturants.

The transitions were best fit by the model equation describing a simple two-state transition for all denaturants, under all conditions. This suggests that only the native and fully unfolded forms of the protein are present in significant concentrations at equilibrium. If intermediates are present, they must comprise a small fraction of the total population under all these conditions.

Kinetic Studies. Although the equilibrium studies suggest that the folding of IFABP follows a two-state model, kinetic studies were needed to test this hypothesis further. Both fluorescence and absorbance data were collected to determine the transient response of apo-IFABP to denaturing and refolding conditions using GdnHCl as the denaturant. A representative kinetic trace of the change in fluorescence for an unfolding "jump" from 0 to 2 M GdnHCl at pH 7.2 and 20 °C is shown in Figure 5A. The fit of these data to a single-exponential phase was inadequate (Figure 5B) whereas two-exponential phases gave a good fit (Figure 5C). The rate of the slow unfolding phase was designated τ_{1U} and that of the fast unfolding phase τ_{2U}. Similar rates were found for the unfolding transition followed by absorbance. Further experiments showed that these two phases were observed for all unfolding transitions and that the total amplitude change observed by fluorescence for these phases accounted for the entire amplitude expected for the transition from equilibrium studies in the stop-flow instrument (Figure 6 and Table I). The calculated ΔG_{H_2O} (5.71 kcal mol^{-1}) and midpoint (1.32 M) agree very well with the GdnHCl-induced unfolding transition monitored by other methods.

The refolding of apo-IFABP as monitored by fluorescence required a two-exponential fit as well. However, the observed rates did not correspond to those determined for unfolding, and the observed amplitude change did not account for the

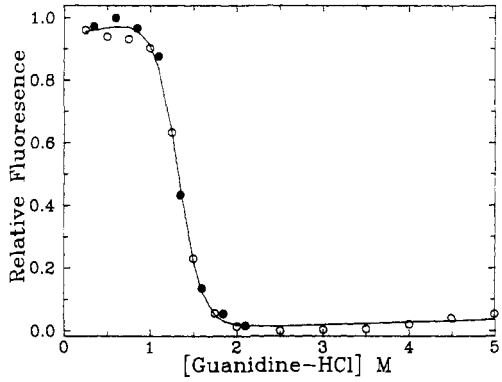

FIGURE 6: Equilibrium unfolding transition of apo-IFABP monitoring the GdnHCl-induced fluorescence change using the Applied Photophysics stop flow. Values of A_∞ were determined from fits to a biphasic exponential equation as described under Materials and Methods from both folding (●) and unfolding (○) transitions and scaled from 0 to 1 as described under Materials and Methods. The unfolding experiments mixed, at a ratio of 1:5, 120 μM apo-IFABP in 20 mM potassium phosphate and 0.1 mM EDTA, pH 7.2, with solutions containing various amounts of GdnHCl in 20 mM potassium phosphate and 0.1 mM EDTA, pH 7.2, resulting in the final concentrations of GdnHCl shown. Similarly, the folding experiments mixed at a ratio of 1:5 120 μM apo-IFABP in 2 M GdnHCl, 20 mM potassium phosphate, and 0.1 mM EDTA, pH 7.2, with solutions containing various amounts of GdnHCl in 20 mM potassium phosphate and 0.1 mM EDTA, pH 7.2, to give the final concentrations of GdnHCl shown. The final concentration of apo-IFABP was 20 μM for all experiments. The line describes the fit to a two-state model as described under Materials and Methods.

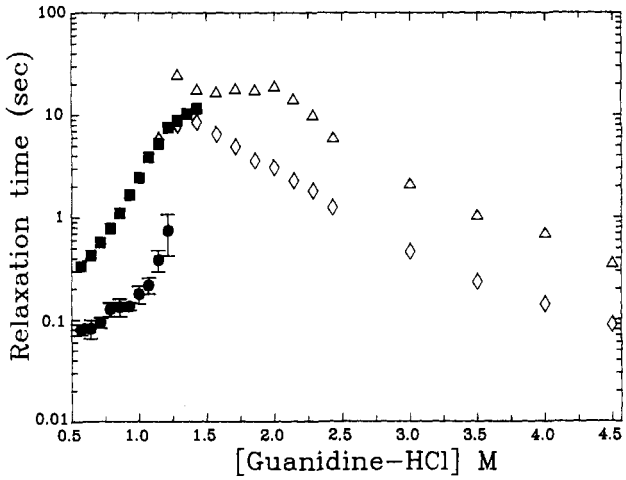

FIGURE 7: Dependence of the observed relaxation times ($1/k_i$) on the final GdnHCl concentration. (■) and (●) correspond to the slow and fast phases of refolding, τ_{1R} and τ_{2R}, respectively. (△) and (◇) correspond to the slow and fast phases of unfolding, τ_{1U} and τ_{2U}, respectively. Error bars shown are one standard error for at least five separate determinations. If no error bar is shown, one standard error is enclosed by the size of the symbol. Conditions for refolding and unfolding are described in Figure 6, except that the final concentrations of apo-IFABP for this experiment were either 10 or 20 μM due to changes in starting concentrations of IFABP and/or different mixing ratios.

expected amplitude change at equilibrium, implying the existence of at least one additional phase occurring in the dead time of the instrument. The observed phases were designated τ_{1R} for the slow refolding phase and τ_{2R} for the fast folding phase.

The GdnHCl concentration dependence of the relaxation times and amplitudes of these phases was determined from a series of unfolding and refolding jumps to various final concentrations. A semilogarithmic plot of the relaxation times as a function of GdnHCl concentration is shown in Figure 7. The observed amplitudes of these phases, scaled relative to the

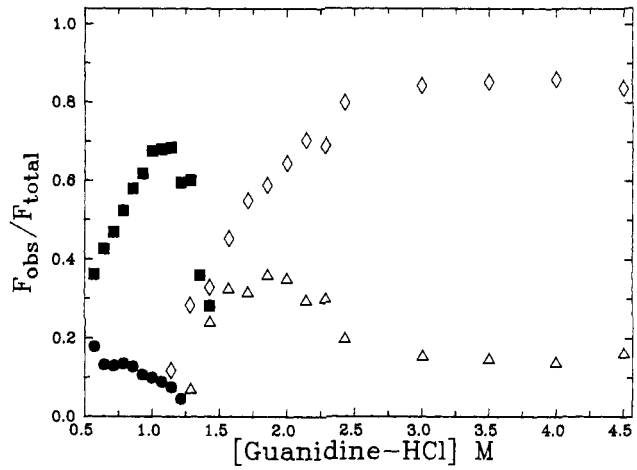

FIGURE 8: Observed amplitudes for the phases observed in Figure 5 normalized to the expected amplitude change at equilibrium. (■) and (●) are the fractional amplitudes of the slow and fast phases of refolding, respectively. (△) and (◇) are the fractional amplitudes of the slow and fast phases of unfolding, respectively. Experimental conditions are described in the legend to Figure 7.

expected amplitude change, are shown in Figure 8. The amplitudes and rates of the unfolding process can be explained by a simple, stepwise process of protein denaturation. The τ_{1R} phase of refolding and the τ_{2U} phase of unfolding connect smoothly, in terms of both relative amplitude and rate, implying that these two phases may correspond to the same physical structures. However, the requirement for at least one additional phase for the folding process and the changes in relative amplitudes of the observed phases show that the folding process is much more complicated than a simple stepwise pathway (see Discussion).

The amplitudes and relaxation times for both unfolding and refolding were independent of the protein concentration over the range of 5–20 μM (data not shown). Therefore, over this concentration range, the reactions are unimolecular and reflect actual protein folding, rather than dimerization or other higher order aggregation. At higher protein concentrations, 20–60 μM, transient reversible aggregation appears to occur, leading to the presence of an additional, much slower, phase during refolding. At still higher final protein concentrations (>60 μM), precipitation occurs during the refolding process. This precipitate can be redissolved only by returning the protein to denaturing conditions. If the precipitated protein is then diluted to less than 60 μM while maintaining the GdnHCl concentration at denaturing concentrations, and the denaturant subsequently removed either by further dilution or by exhaustive dialysis, normal refolding occurs. The protein concentration dependent precipitation is further evidence for the existence of an intermediate or intermediates that can aggregate during the folding process. The unfolding transition is much less affected by final protein concentration, so long as the concentration of GdnHCl is sufficient to completely unfold the protein (>1.8 M).

The four tyrosine residues of IFABP do not appear to contribute to the fluorescence emission spectrum of the protein in either the denatured or the native states, even if a lower excitation wavelength (285 nm) is used to increase their contribution. Since the changes in fluorescence *may* be related only to whether the tryptophans are in their final structural position and not to when the secondary structural backbone is formed, we attempted to follow secondary structure formation by stopped-flow CD. Due to severe mechanical and electronic problems encountered for stopped-flow CD with this instrumentation (see Materials and Methods), only a single

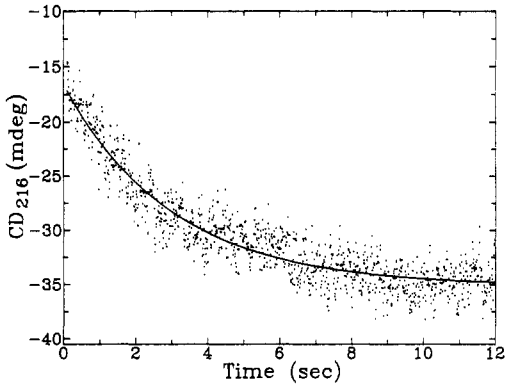

FIGURE 9: Plot of the change in ellipticity at 216 nm for a refolding jump from 2 to 1 M GdnHCl measured by stopped-flow CD. The path length of the cell was 1 cm. The left chamber contained 4 μM apo-IFABP in 2 M GdnHCl, 20 mM potassium phosphate, and 0.1 mM EDTA at pH 7.2. The right chamber contained 20 mM potassium phosphate and 0.1 mM EDTA at pH 7.2. A 1:1 mixing ratio resulted in a final concentration of 1 M GdnHCl and 2 μM IFABP. A total of 24 transients were accumulated to monitor the transition. The line shown is the fit to a single-exponential decay.

refolding transition can be reported. This transition, from 2 M GdnHCl to approximately 1 M GdnHCl (Figure 9), gave a τ value (3.01 ± 0.4 s, average of 4 sets of 24 transients) similar to that of τ_{1R} (2.45 ± 0.11 s, average of 5 transients, Figure 7) for an equivalent concentration jump. Further, the observed amplitude of the transition (18.6 mdeg) is about 68% of the expected amplitude change for this protein concentration (27 mdeg), similar to the relative amplitude of the τ_{1R} phase of fluorescence (68%, Figure 8). A fit to two exponentials did not result in a significant improvement over the single-exponential fit, but the data are probably inadequate to define a second phase. Still, it is encouraging to find such similarity in results obtained with two optical methods, suggesting that the observed fluorescence changes may truly represent changes in the overall secondary structure of the protein, rather than local changes in tryptophan ring position after the secondary structure is completely formed.

Discussion

IFABP appears to be an excellent model system to study protein folding. The structure of IFABP is extremely unusual in that is has no true hydrophobic core. Rather the hydrophobic amino acid side chains project into a large solvent-filled internal cavity. Solvent displacement may be important in ligand binding (Sacchettini et al., 1989b). Given the unusual degree of solvent accessibility to the core of the protein and the lack of disulfide bonds, the stability of IFABP is remarkable. The protein is stable between pH 3 and pH 12 and to temperatures >70 °C at pH 7.2 and low ionic strength (data not shown). The folding and unfolding transitions appear to be completely reversible at low protein concentrations, and the processes are not complicated by the presence of either prolines or cysteines since the protein does not contain them. It is clear that the primary sequence of this protein encodes a folding motif that is very stable in solution and whose formation is kinetically rapid. However, the interpretation of these data in terms of overall structural stability and the specific structure(s) of intermediates in the folding pathways remains difficult.

Equilibrium Studies. One problem in the use of denaturing agents to study protein stability is the difficulty in assessing the true free energy of unfolding in the absence of denaturant (Tanford, 1968; Pace, 1975; Schellman, 1978). Several different methods of calculating ΔG_{H_2O} have been proposed and discussed (Tanford, 1964, 1968; Aune & Tanford, 1969; Pace, 1975; Schellman, 1978). A few recent publications have supported the validity of linear extrapolation to determine this parameter (Schellman, 1978; Santoro & Bolen, 1988; Shortle et al., 1989). When this method is applied to the same protein using different denaturants, only small differences, usually less than 2 kcal mol^{-1}, are found for ΔG_{H_2O} among the different denaturants (Pace, 1975; Pace & Marshall, 1980; Santoro & Bolen, 1988). This is not the case for IFABP, suggesting that the linear extrapolation model is incorrect for this protein. The 5 kcal mol^{-1} difference for ΔG_{H_2O} among the different denaturants is by far the greatest difference yet reported. The use of the other methods [reviewed by Tanford (1968) and Pace (1975)] to determine ΔG_{H_2O} did not reduce this difference. The stability of IFABP toward pH and temperature would seem to indicate that 10 kcal mol^{-1} might be the true stability of the protein in the absence of denaturant. If this is true, GdnHCl and KSCN must somehow reduce the overall stability of the protein by an unknown mechanism. Alternatively, if 5 kcal mol^{-1} is the true ΔG_{H_2O}, urea, dimethylurea, and GdnSCN must somehow increase the stability of the protein by an additional 5 kcal mol^{-1}. This phenomenon may be related (1) to the large, solvent-filled internal cavity of IFABP (approximately 500 Å^3; J. Sacchettini, personal communication), (2) to high-affinity binding site(s) for specific denaturants that greatly decrease or increase the overall stability of the protein, or (3) to differing susceptibilities of the complex intrastrand hydrogen-bond network that forms the structure of IFABP to different denaturants.

It has been shown that GdnHCl, at low nondenaturing concentrations, appears to bind at the surface of α-chymotrypsin, whereas urea binds both in the interior hydrophobic spaces and on the surface at low nondenaturing concentrations (Hibbard & Tulinsky, 1978). The large interior cavity might allow the binding of GdnHCl on the interior surface as well, causing an anomalous increase in the effectiveness of GdnHCl as a denaturant. The $GdnH^+$ ion is considered to be the likely entity that causes the unfolding of proteins in GdnHCl (Tanford, 1970). Although urea and $GdnH^+$ could both be binding in the interior of IFABP, the binding of $GdnH^+$ to the interior of IFABP would effectively bury a charge within the protein (a greatly destabilizing event). The chaotropic agent KSCN may be able to act in a similar fashion.

The method of linear extrapolation to determine ΔG_{H_2O} assumes many weak binding sites for denaturant on the protein (Schellman, 1978). If a single or a few high-affinity binding site(s) for GdnHCl (or $GdnH^+$) exist that lower the overall protein stability much more than would be expected from weak binding sites, the extrapolation method would give anomalously low estimates of ΔG_{H_2O}. There is some evidence in the literature for high-affinity binding sites for GdnHCl (Bismuto & Irace, 1988; Liu & Tsou, 1987). Another member of this protein superfamily, β-lactoglobulin, was though to have a high affinity site for GdnHCl that increases the stability of β-lactoglobulin by as much as 3.9 kcal mol^{-1}, depending on the method of extrapolation used (Greene & Pace, 1974; Pace & Marshall, 1980). It is certainly possible that a high-affinity site on the native enzyme that decreases the overall stability could exist for IFABP. Alternatively, a high-affinity site for GdnHCl on the unfolded form of the protein would have the same effect, lowering the ΔG_{H_2O}. Similarly, a high-affinity site for KSCN (SCN^-) may be present.

A more typical result for the high-affinity binding of a molecule is the stabilization of the native structure, as in the case for the binding of fatty acid to IFABP. It may be that

the binding of urea or dimethylurea to the interior cavity of IFABP stabilizes the native structure. Hibbard and Tulinsky (1978) have speculated that the reason that urea is generally a less effective denaturant than GdnHCl is that urea has both stabilizing as well as destabilizing interactions with proteins. These binding models would all result in curved plots of ΔG versus denaturant concentration, but the range of concentration over which this curvature exists is not experimentally observable under these conditions.

As stated above, the interior of IFABP is unusual in that there is a large included volume that is contained within rather than occupied by the protein. The two antiparallel β-sheets, each formed by complex hydrogen-bonding interactions between five antiparallel β-strands arranged in a +1, +1, +1, +1, +1 motif (Richardson, 1977), enclose this interior cavity (see Figure 1). The observed variation in ΔG_{H_2O} may reflect differences in the permeability of the β-clam structure to the various solvents (denaturants) and/or differing susceptibilities of the hydrogen-bond network to disruption by these compounds. However, none of these hypotheses can easily explain the increased ΔG_{H_2O} found for GdnSCN. It is not clear why a combination of the two denaturants that results in a low ΔG_{H_2O} would give an estimate for ΔG_{H_2O} similar to that found for urea and dimethylurea. Further study of these phenomena might provide more information on how these denaturants actually unfold proteins, and perhaps explain the differences in ΔG_{H_2O} among the denaturants.

The structures of apo-IFABP and holo-IFABP are extremely similar (Sacchettini et al., 1989a,b). As such, it has been difficult to assess the contribution of ligand binding to overall structural stability. The 2.5 kcal mol^{-1} increase in ΔG_{H_2O} in the presence of ligand for studies in either GdnHCl or urea is the first measure of the increase in protein stability associated with ligand binding for any member of this protein family. The location of the ligand within the β-clam causes the methylene chain of the fatty acid to lie in a hydrophobic "cradle" (Sacchettini et al., 1989b) composed of aromatic and hydrophobic side chains. In the apoprotein, this space is occupied by seven additional ordered water molecules. Although part of the increased stability is caused by the formation of a salt bridge between Arg-106 and the carboxylate group of the fatty acid, some contribution to the overall stability of the protein must be caused by these hydrophobic interactions.

Kinetic Models. (1) Unfolding Reaction. The simplest model for the unfolding reaction requires only a sequential breakdown of two different regions of the protein, each region containing one of its two tryptophans[3] (Scheme I).

Scheme I

$$N \xrightarrow{\tau_{2U}} I \xrightarrow{\tau_{1U}} U$$

This model is particularly attractive since the two tryptophans (Trp-6 and Trp-82) are at opposite "corners" of the β-clam (Figure 1), and perhaps these regions of the protein could unfold independently. Even if this hypothesis is correct, the data collected thus far do not allow us to determine which region is more stable. Other hypotheses are certainly possible, including more global "molten globule" like intermediates, but a sequential model is the simplest and most easily tested. It is unfortunate that our attempts to use stop-flow CD to follow the unfolding reaction have been unsuccessful to date, since information on the remaining secondary structure present during denaturation might help distinguish between the molten globule and sequential models.

Scheme II

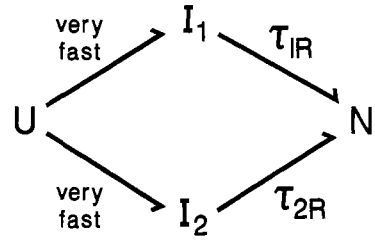

(2) Refolding Reaction. The refolding reaction of IFABP is much more complicated. A minimum of three phases are present, with the relative amplitudes of these phases dependent on the final GdnHCl concentration. The proportion of the total amplitude that is not observed and the amplitude of the τ_{2R} phase increase with decreasing GdnHCl concentration, whereas the amplitude of the τ_{1R} phase decreases with decreasing GdnHCl concentration. These amplitude changes can be explained by the presence of two potential folding pathways, and that the proportion of protein molecules following any particular pathway changes with the final GdnHCl concentration (Scheme II).

In this model, the upper pathway predominates at higher final concentrations of GdnHCl (greater amplitude in phase τ_{1R}), whereas the lower branch predominates for jumps to lower final concentrations of GdnHCl (greater amplitude in phase τ_{2R}). For both pathways, there is an initial rapid step accounting for the missing fraction of the total amplitude change, followed by the slower observed phases. The initial rapid step could be a hydrophobic collapse of some sort, with different fractions of the total protein structure collapsed in the two intermediates I_1 and I_2. Presumably, the I_2 is either larger or more nativelike than the I_1 fragment since more of the expected amplitude change occurs in the rapid, unobserved phase. Since the 2 to 1 M GdnHCl jump, as monitored by CD, shows that some secondary structure appears very rapidly, followed by the assembly of the remaining secondary structure, these intermediates might be considered nuclei for further structure formation. It may be that the presence of higher concentrations of GdnHCl prevents the collapse of denatured IFABP to a larger I_2 fragment.

In summary, IFABP appears to be a very useful model system to study the stability of β-sheet structures and fast steps in protein folding. Further experiments (e.g., site-directed mutagenesis to replace each of the two tryptophans to determine which phases, if any, are associated with a particular tryptophan) are required to determine the forces that stabilize the β-clam and to determine the structures of the intermediates on the protein folding and unfolding pathways.

Registry No. Oleic acid, 112-80-1.

[3] Note that the fits of the kinetic data by a double-exponential equation would be that of a parallel model for unfolding as well. Since the rate constants for the two steps differ only by a factor of 3, this equation does not describe a sequential process correctly. The equation for a sequential model under these conditions is much more complicated (Tandford, 1970). Although both the rates and amplitudes for the two observed phases are different for the two models, both models fit the data equally well. Since the actual mechanism of unfolding is not currently known, we have presented the fit of these data to the simpler model.

References

Aune, K., & Tanford, C. (1969) *Biochemistry 8*, 4579–4590.
Baldwin, R. L. (1989) *Trends Biochem. Sci. 14*, 291–294.
Bernlohr, D. A., Angus, C. W., Lane, M. D., Bolanowski, M. A., & Kelly, T. J. (1984) *Proc. Natl. Acad. Sci. U.S.A. 81*, 5468–5472.
Bismuto, E., & Irace, G. (1988) *Int. J. Pept. Protein Res. 32*, 321–325.

Böhmer, F.-D., Kraft, R., Otto, A., Wernstedt, C., Hellman, U., Kurtz, A., Muller, T., Rohde, K., Etzold, G., Lehmann, W., Langen, P., Heldin, C. H., & Grosse, R. (1987) *J. Biol. Chem. 262*, 15137–15143.

Brandts, J. F., Halvorson, H. R., & Brennan, M. (1975) *Biochemistry 14*, 4953–4963.

Gordon, J. I., Alpers, D. H., Ockner, R. K., & Strauss, A. W. (1983) *J. Biol. Chem. 258*, 3356–3363.

Greene, R. F., & Pace, C. N. (1974) *J. Biol. Chem. 249*, 5388–5393.

Heuckeroth, R. O., Birkenmeier, E. H., Levin, M. S., & Gordon, J. I. (1987) *J. Biol. Chem. 262*, 9709–9717.

Hibbard, L. S., & Tulinsky, A. (1978) *Biochemistry 17*, 5460–5468.

Huber, R., Schneider, M., Mayr, I., Muller, R., Deutzmann, R., Suter, F., Zuber, H., Falk, H., & Kayser, H. (1987) *J. Mol. Biol. 198*, 499–515.

Hunt, C. R., Ro, J. H.-S., Dobson, D. E., Min, H. Y., & Spiegelman, B. M. (1985) *Proc. Natl. Acad. Sci. U.S.A. 83*, 3786–3790.

Ishaque, A., Hofmann, T., Rhee, S., & Eylar, E. H. (1982) *J. Biol. Chem. 257*, 592–595.

Johnson, W. C. (1988) *Annu. Rev. Biophys. Biophys. Chem. 17*, 145–166.

Jones, T. A., Bergfors, T., Sedzik, J., & Unge, T. (1988) *EMBO J. 7*, 1597–1604.

Li, E., Demmer, L. A., Sweetser, D. A., Ong, D. E., & Gordon, J. I. (1986) *Proc. Natl. Acad. Sci. U.S.A. 83*, 5779–5783.

Liu, W., & Tsou, C.-L. (1987) *Biochim. Biophys. Acta 916*, 455–464.

Lowe, J. B., Sacchettini, J. C., Laposata, M., McQuillan, J. J., & Gordon, J. I. (1987) *J. Biol. Chem. 262*, 5931–5937.

Mannervik, B. (1982) *Methods Enzymol. 87*, 370–389.

Monaco, H. L., Zanotti, G., Spadon, P., Bolognesi, M., Sawyer, L., & Eliopoulos, E. E. (1987) *J. Mol. Biol. 197*, 695–706.

Motulsky, H. J., & Ransnas, L. A. (1987) *FASEB J. 1*, 365–374.

Newcomer, M. E., Jones, T. A., Aqvist, J., Sundelin, J., Eriksson, U., Rask, L., & Peterson, P. A. (1984) *EMBO J. 3*, 1451–1454.

Olins, P. O., & Rangwala, S. H. (1990) *Methods Enzymol. 185*, 115–119.

Pace, C. N. (1975) *CRC Crit. Rev. Biochem. 3*, 1–43.

Pace, C. N. (1986) *Methods Enzymol. 131*, 266–280.

Pace, C. N., & Marshall, H. F. (1980) *Arch. Biochem. Biophys. 199*, 270–276.

Paul, C., Kirschner, K., & Haenisch, G. (1980) *Anal. Biochem. 101*, 442–448.

Richardson, J. S. (1977) *Nature 268*, 495–500.

Sacchettini, J. C., Meininger, T. A., Lowe, J. B., Gordon, J. I., & Banaszak, L. J. (1987) *J. Biol. Chem. 262*, 5428–5430.

Sacchettini, J. C., Gordon, J. I., & Banaszak, L. J. (1988) *J. Biol. Chem. 263*, 5815–5819.

Sacchettini, J. C., Gordon, J. I., & Banaszak, L. J. (1989a) *Proc. Natl. Acad. Sci. U.S.A. 86*, 7736–7740.

Sacchettini, J. C., Gordon, J. I., & Banaszak, L. J. (1989b) *J. Mol. Biol. 208*, 327–339.

Sacchettini, J. C., Banaszak, L. J., & Gordon, J. I. (1990) *Cell. Mol. Biochem.* (in press).

Santoro, M. M., & Bolen, D. W. (1988) *Biochemistry 27*, 8063–8068.

Schellman, J. A. (1978) *Biopolymers 17*, 1305–1322.

Shortle, D., Meeker, A. K., & Gerring, S. L. (1989) *Arch. Biochem. Biophys. 272*, 103–113.

Sundelin, J., Anundi, H., Tragardh, L., Eriksson, U., Lind, P., Ronne, H., Peterson, P. A., & Rask, L. (1985a) *J. Biol. Chem. 260*, 6488–6493.

Sundelin, J., Das, S. R., Eriksson, U., Rask, L., & Peterson, P. A. (1985b) *J. Biol. Chem. 260*, 6494–6499.

Sweetser, D. A., Heuckeroth, R. O., & Gordon, J. I. (1987) *Annu. Rev. Nutr. 7*, 337–359.

Tanford, C. (1964) *J. Am. Chem. Soc. 86*, 2050–2054.

Tanford, C. (1968) *Adv. Protein Chem. 23*, 121–275.

Tanford, C. (1970) *Adv. Protein Chem. 24*, 1–95.

Tonomura, B., Nakatani, H., Ohnishi, M., Yamaguchi-Ito, J., & Hiromi, K. (1978) *Anal. Biochem. 84*, 370–383.

Walz, D. A., Wider, M. D., Snow, J. W., Dass, C., & Desiderio, D. M. (1988) *J. Biol. Chem. 263*, 14189–14195.